EFFECT OF ALLOYING ELEMENTS ON GROWTH BEHAVIOR OF INTERMETALLIC COMPOUNDS AT THE COLD-SPRAYED COATING/STEEL INTERFACE DURING IMMERSION IN ALUMINUM MELT

K. Bobzin, M. Öte, S. Wiesner, and L. Gerdt
Surface Engineering Institute, RWTH Aachen University, Aachen, Germany

A. Bührig-Polaczek and J. Brachmann
Foundry Institute, RWTH Aachen University, Aachen, Germany

https://doi.org/10.1007/s40962-017-0205-0

Abstract

The formation of the intermetallic compounds at the interface between cold-sprayed coatings and steel as well as interaction between coatings and aluminum melt was investigated. Coatings of AA7075 (AlZn5.5MgCu) and AA4145 (AlSi10Cu4) were deposited on the sheets of the deep drawing steel DC04. The coated samples were then immersed in the aluminum melt AlSi9Mn at the temperature of $T = 610$ °C for different durations in the range $30\ s < t < 10$ min. The reaction layer growth was examined metallographically and by means of scanning electron microscope with energy-dispersive spectroscopy. Furthermore, the intermetallic phases were identified by X-ray diffraction analysis and characterized by microhardness measurements. For both coatings, β-AlFeSi phases were shown to be the major constituent in the reaction zone. The growth kinetics of the intermetallic phases appeared to be similar for AA4145 and AA7075 coatings, while their morphology was completely different.

Keywords: *high-pressure die casting, coating, cold gas spraying, immersion tests, reaction layer growth*

Introduction

An intelligent lightweight design is of essential interest in modern automotive manufacturing. Hybrid construction is one of the possible solutions. Striving for required lightweight and strength of the car body, structures made of aluminum and steel are particularly desirable from the manufacturing point of view. For decades, aluminum and steel have remained the most significant materials in automotive industry. Joining of these materials, however, is still a challenging task due to dissimilar thermophysical and metallurgical properties and the formation of brittle intermetallic phases. Besides welding and brazing, the high-pressure casting represents another technique for joining dissimilar metals. Casting of gray cast iron liners with aluminum[1] or Al inserts with Mg alloy[2] in the engine crankcase is already state of the art. Pressure casting of aluminum onto a steel insert has been also at the focus of research at RWTH Aachen University in recent years.[3] The cooperation between the foundry institute and industrial partners resulted in a "VarioStruct" prototype of the roof cross-beam of the vehicle.[4] Despite these successes, further improvement of the compound properties is required, as the problem of the brittle intermetallic phases and the gap formation at the aluminum/steel interface has not been completely solved. Due to enormous cooling rates after pressure casting and insufficient wetting of steel by aluminum, it is difficult to achieve a metallurgical bonding at the interface. In order to enable a gap-free material bonding between the steel and the cast aluminum alloy, different coatings for steel inserts are investigated in the current study. The main challenge is the application of coatings with a reliable adhesion on the steel substrate which facilitates metallurgical bonding with the aluminum melt during the pressure casting. In the pressure casting process, the steel insert is heated up to a temperature of $T = 400$–520 °C, while the temperature of the molten aluminum is about $T = 700$ °C.[3] Therefore, Al-based alloys AA4145 and AA7075 with low solidus temperature were selected to enable a partial melting of the coating

deposited on the steel to achieve a metallurgical bonding with cast alloy.

Recently, a number of studies examined the chemical composition and the growth behavior of intermetallic phases during hot dip aluminizing of steel.[5–9] Some of them were focused on the effects of alloying elements on the morphology and growth kinetics of the intermetallic compounds.[6,7] The control of the reaction zone at the interface between aluminum and steel is of special interest regarding the mechanical properties of the joint, in particular its strength. For a silicon containing aluminum cast alloy, the formation of $Al_{4.5}FeSi$ and $Al_8(Fe,M)_2Si$ with M = Mn or Cu at the steel interface was shown to be predominantly in the immersion tests.[9,10] In the current study, formation and growth of the intermetallic compounds at the interface coating/steel and the interaction between melt and coating, due to the possible partial melting of the coatings, are investigated. The effects of the alloying elements of the coatings such as Si, Mg, Cu and Zn on the morphology and growth kinetics of intermetallic phases are in the focus of this study.

Experimental

The experimental procedure consisted of a cold spraying process, immersion tests or heat treatment of coated samples and analysis. The principle scheme of the experimental setup is shown in Figure 1.

Cold Spraying

In the present study, the conventional cold rolled deep-draw steel DC04 was selected as substrate material. The untreated steel in the as-rolled condition as well as after grit blasting was analyzed to determine the impact of surface quality and spray parameters on the coating formation. Alumina with the grit sizes of F80 was used as blasting abrasive. Prior to cold spraying, a punch press was used to form the sheet steel into rectangular plates ($200 \times 30 \times 2$ mm^3). Due to the low melting ranges of these alloys, AA4145 and AA7075 were chosen as feedstock materials for coating application to achieve a metallurgical bonding with the aluminum melt during the high-pressure die casting. The compositions of the materials are given in Table 1. AA4145 powder with a size distribution of $-45 + 15$ µm and AA7075 powder with a size distribution of $-63 + 20$ µm were delivered by TLS Technik GmbH (Bitterfeld, Germany). The Kinetics 8000 Cold spray system from Oerlikon Metco (Pfäffikon, Switzerland) was used for depositing Al-based coatings with nitrogen as process and carrier gas.

The process parameters for cold gas spraying of AA4145 and AA7075 alloys are given in Table 2. The number of deposition passages was 4 for both coatings.

Immersion Test

For immersion tests, a Trimal 37 (AlSi9Mn) cast alloy from Trimet Aluminium SE (Essen, Germany) with a total weight of about $m = 6$ kg was melted in a clay bonded graphite crucible by August Gundlach KG (Großalmerode, Germany). Considering the ratio of the mass between the immersed samples and molten aluminum, we can assume that the possible changes in the bath composition, if any, are marginal. In order to lower the hydrogen content, the melt was degassed using a chemically inert Argon 4.8. Oxides on the melt surface, which could restrain the wettability of the steel sheets, were mechanically removed with a pouring ladle. The temperature of the melt was controlled before and after the immersion of the samples by means of k-type thermocouple and was held at

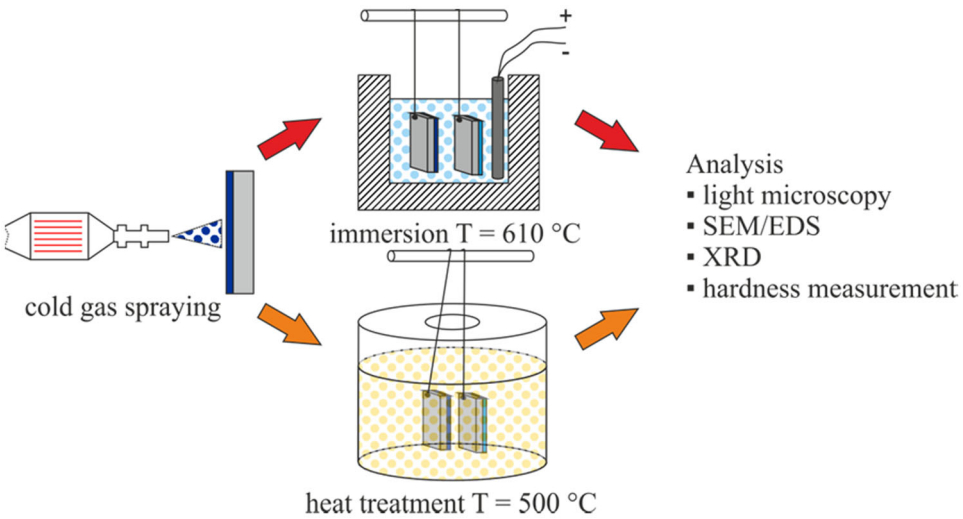

Figure 1. Experimental sequence: cold spraying, immersion tests, heat treatment and analysis.

Table 1. Chemical composition of the substrate, cast alloy and filler materials (wt%)

	Si	Mn	Mg	C	S	P	Cu	Al	Fe	Zn
DC04		0.4		0.08	0.03	0.03			Bal.	
AA4145	10.0						4.00	Bal.		
AA7075	0.4	0.3	2.5				1.60	Bal.		5.5
Trimal 37	9.0	0.4	0.08				0.03	Bal.	0.15	

Table 2. Spraying parameters for AA4145 and AA7075 coatings

	AA4145, AA7075
Gas temperature (°C)	490
Process gas flow, N_2 (m^3/h)	60
Carrier gas flow, N_2 (m^3/h)	3.0
Spray distance (mm)	25
Transverse movement velocity (mm/s)	200

$T = 610 \pm 4$ °C using an electric holding furnace. The coated samples were then immersed in the aluminum melt for five different times varying between $t = 30$ s and $t = 10$ min.

Heat Treatment in Fluidized Sand Bath

For the high-pressure die casting process of aluminum, it was shown that the maximum temperature at the surface of the steel insert during the process is in the range of $T = 500$–520 °C.[11] In order to simulate the temperature regime of the process, the coated samples were heat-treated in a fluidized sand bath furnace at the temperature of $T = 500$ °C for $t = 30$ s to $t = 10$ min.

Characterization

In order to characterize the coating, the cold-sprayed samples were metallographically prepared and examined in terms of their microstructure. The coating thickness was measured on the cross sections using an optical microscope by Carl Zeiss with Axio Vision image analysis tool. A microhardness tester Fisherscope HM2000 by Helmut Fischer GmbH (Sindelfingen-Maichingen, Germany) was used for the examination of the hardness of the reaction zone at the interface coating/steel with a load of $m = 5$ g. In order to identify the reaction layers at the interface between steel and aluminum alloy after heat treatment, an energy-dispersive spectroscopy analysis was performed by means of the scanning electron microscope Zeiss Leo 1530 with the EDS device Bruker Quantax 200. The crystal structure of the compound layers was identified by X-ray diffractometer Seifert XRD 3003 (GE Sensing & Inspection Technologies GmbH, Hürth, Germany) using monochromatic Cu Kα radiation.

The mean thickness of the intermetallic compounds was determined from three micrographs of the immersed or heat-treated samples produced by scanning electron microscope using electron backscatter diffraction detector (SEM/RBSD), Figure 2. First, the area of the section corresponding to the reaction zone was identified by segmentation and binarization of the image. The binarization of the images was performed by setting a threshold value. The mean threshold was in the range $65 < T < 125$ for true color 24 bit image. After binarization process, each image was visually compared with the original one to determine the optimum threshold setting. Therefore, the estimated d values were sensitive to threshold; however, the sensitivity was negligible even for thin intermetallic layers. After the image processing, the mean thickness d was calculated as a ratio between the reaction zone area A and its length L:

$$d = \frac{A}{L} \qquad \text{Eqn. 1}$$

It should be mentioned that the area of the whole reaction zone which consists of different intermetallic layers was considered.

Results and Discussion

The deposition tests showed that for the AA4145 alloy it was difficult to achieve a sufficient bonding on untreated substrates. After grit blasting the steel surface with alumina F80, a coating with a thickness of about $d = 60$ µm was deposited, Figure 3a. The porosity of the AA4145 coating was about $p = 2\%$. Coating of AA7075 alloy could be deposited by cold spraying on the steel substrate without previous surface treatment. Figure 3b shows the cross section of the AA7075 coating. The feedstock material exhibited a good plasticity resulting in a tight bonding between particles. The coatings of AA7075 have a porosity of about $p = 0.5\%$. The thickness of the coating was of about $d = 150$ µm.

REM/EDS Analysis

After the heat treatment at the temperature $T = 500$ °C, no reaction zone was observed on SEM/EBSD cross sections

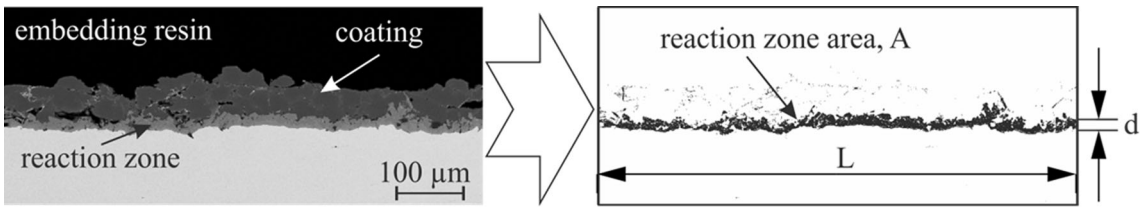

Figure 2. Scheme for determination of the reaction zone thickness d by binarization.

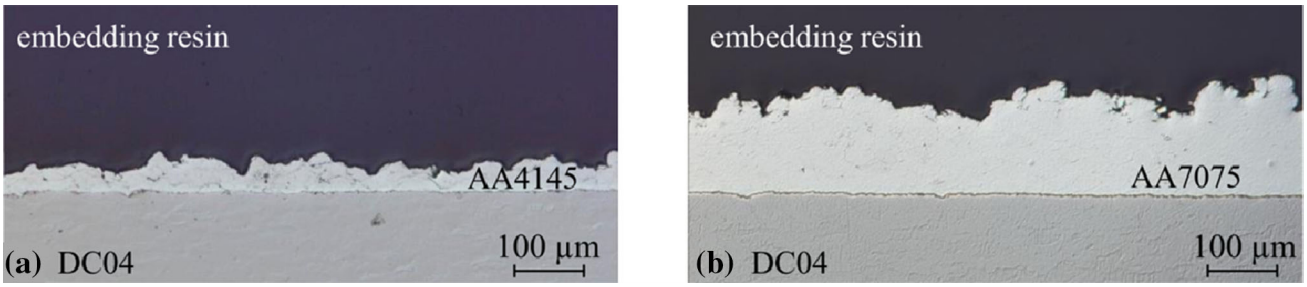

Figure 3. Cross section of (a) AA4145 coating, (b) AA7075 coating after deposition.

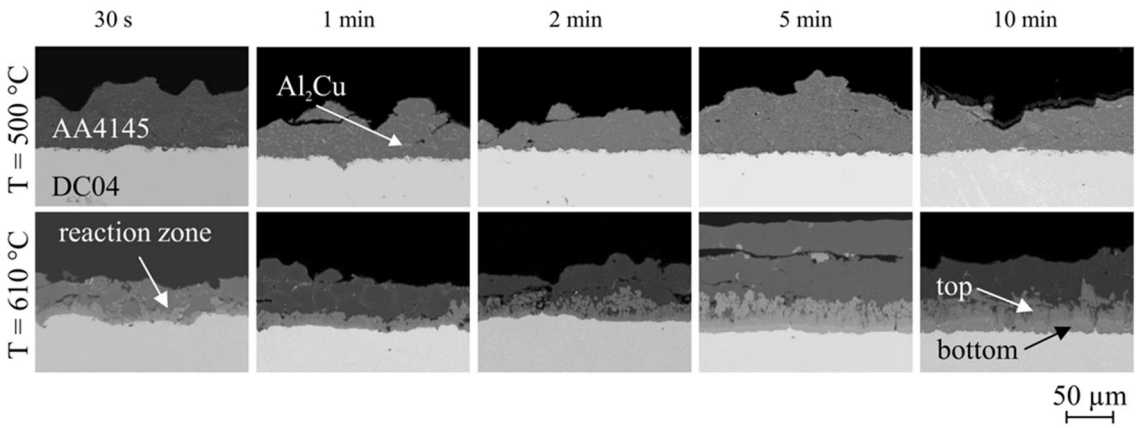

Figure 4. SEM/RBSD cross-sectional micrograph of the reaction zone between AA4145 coating and steel after heat treatment at T = 500 °C and after immersion at the temperature T = 610 °C.

for the AA4145 coating even after a long annealing time of $t = 10$ min. Some precipitations were detected at the particle boundaries. The EDS analysis pointed out that the precipitations at the particle boundaries have a composition corresponding to the Al_2Cu intermetallic phase, Figure 4. No considerable changes of the coating morphology or microstructure were observed with increasing heat treatment time.

After the immersion of the coated samples in the aluminum melt at $T = 610$ °C, a reaction zone at the interface between the AA4145 coating and steel was observed, Figure 4. A densification of the coating occurred after longer immersion in the aluminum melt, possibly due to the sintering effect at the interfaces between the particles. No bonding between AA4145 coating and aluminum melt could be detected. Already after a short immersion time of $t = 30$ s, a reaction zone has formed at the interface between coating and steel. The morphology of the reaction zone is relatively homogenous. Considering the structure of the reaction zone observed at the SEM micrographs, it was conditionally subdivided in bottom and top layers. The results of the EDS analysis indicated the formation of $(Al,Si)_2Fe$ and Al_5Fe_2 at the interface with the steel, Table 3. The chemical composition of the top layer differs

Table 3. Chemical composition of different phases in the reaction zone of AA4145 alloy after immersion time of t = 10 min from EDS analysis in wt%

Layer		Possible IMP	Al	Fe	Si
Continuous	Bottom layer	$(Al,Si)_2Fe$/ Al_5Fe_2	45.60	53.78	0.61
	Top layer	$Al_{12}Fe_5Si$/ Al_8Fe_2Si/ Al_5FeSi	50.93	41.61	7.44
		Al_2Cu			

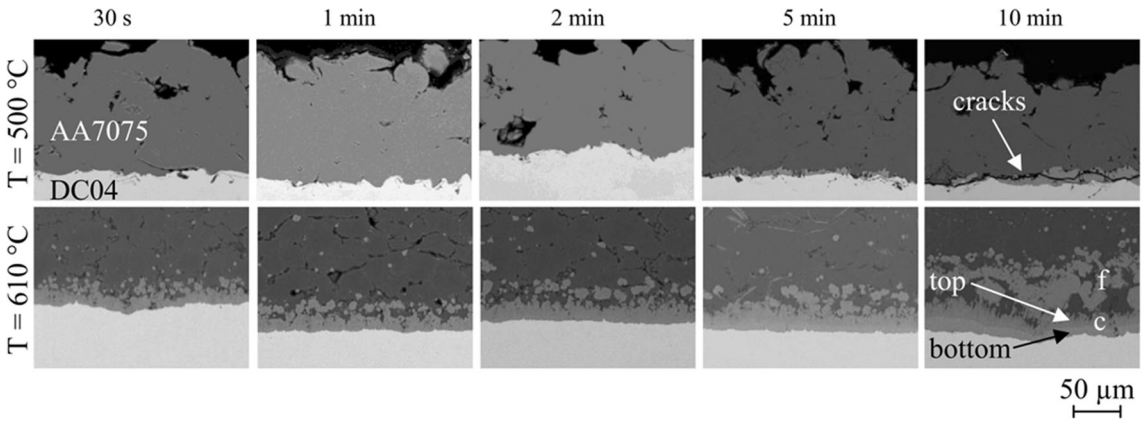

Figure 5. SEM/RBSD cross-sectional micrograph of reaction zone between coating AA7075 and steel after heat treatment at $T = 500$ °C and immersion at the temperature $T = 610$ °C.

over its thickness, corresponding to the three different intermetallic phases $Al_{12}Fe_5Si$, Al_8Fe_2Si and Al_5FeSi. Al_2Cu intermetallic phases were detected at the particles boundaries at short immersion times between $t = 30$ s and $t = 1$ min. With increasing immersion time, the Al_2Cu particles dissolve and the copper content in the coating decreases drastically possibly due to the diffusion toward the aluminum melt with low copper content.

For the AA7175 coating, the formation of the reaction zone at the interface with the steel could be detected after the heat treatment at $T = 500$ °C for a dwell time of $t = 2$ min. After $t = 10$ min, the mean thickness of the reaction zone was about $d_{RZ} = 6$ µm. The EDS analysis revealed the formation of the Al_5Fe_2 intermetallic phase. Due to the rapid cooling after the heat treatment in the fluidized sand bath furnace, thermally induced crack formation occurred locally in the reaction zone, Figure 5.

During immersion tests, the formation of the reaction zone for AA7075 coating was similar to that of the AA4145 coating at the earlier reaction stages when the immersion time was less than one minute. However, with increasing immersion time, the morphology of reaction zone became completely different. The intermetallic layers in the case of the AA7075 coating showed stronger irregularities in their morphology. As shown in Figure 4 for $t = 10$ min, the reaction zone can be subdivided in two zones: a continuous one, adjacent to the substrate surface and labeled with "c" and a flaky one "f" which is separated from the first one. Additionally, the continuous zone can be further subdivided into two layers, which differ from each other in their chemical composition. According to EDS analysis, the thin layer at the steel interface has a composition corresponding to that of $Fe(Al,Si)_2$ or Al_5Fe_2, Table 4. For the top layer, the formation of $Al_{12}Fe_5Si$ can be observed. In the flaky layer, the composition of the intermetallic compounds varies slightly and corresponds to that of Al_8Fe_2Si or Al_5FeSi phases.

A special characteristic of the reaction zone in the case of AA7075 is a low-iron region between the so-called continuous and flaky zones. In Figure 6, it can be seen in the line scan of the main coating and steel components that some AlFeSi particles are located at a considerable large distance from the interface coating/steel in the coating. The sloping edge of the iron content toward the coating is interrupted with some gaps indicating phases with low-iron content. For the coating of AA7075 alloy, a metallurgical bonding between aluminum melt and coating was observed at different places after immersion times of more than $t = 5$ min. During the high-pressure die casting process, the dwell time of the contact between coated steel insert and aluminum melt at elevated temperatures is shorter, whereby the melt temperature is with about $T = 700$ °C higher than during the immersion tests. Considering these points, a metallurgical bonding can be expected for AA7075 coating in high-pressure casting process.

Table 4. Chemical composition of different phases in the reaction zone of AA7075 alloy after immersion time of $t = 10$ min from EDS analysis in wt%

Layer	Sublayer	Possible IMPs	Al	Fe	Si	Mg	Zn	Cu
A: Continuous	Bottom layer	$(Al,Si)_2Fe/Al_5Fe_2$	45.03	52.38	1.22	0.41	0.87	0.08
	Top layer	$Al_{12}Fe_5Si$	49.05	42.63	7.14	0.43	1.60	1.79
B: Flaky	–	Al_8Fe_2Si/Al_5FeSi	52.89	33.99	6.31	0.82	1.71	1.98

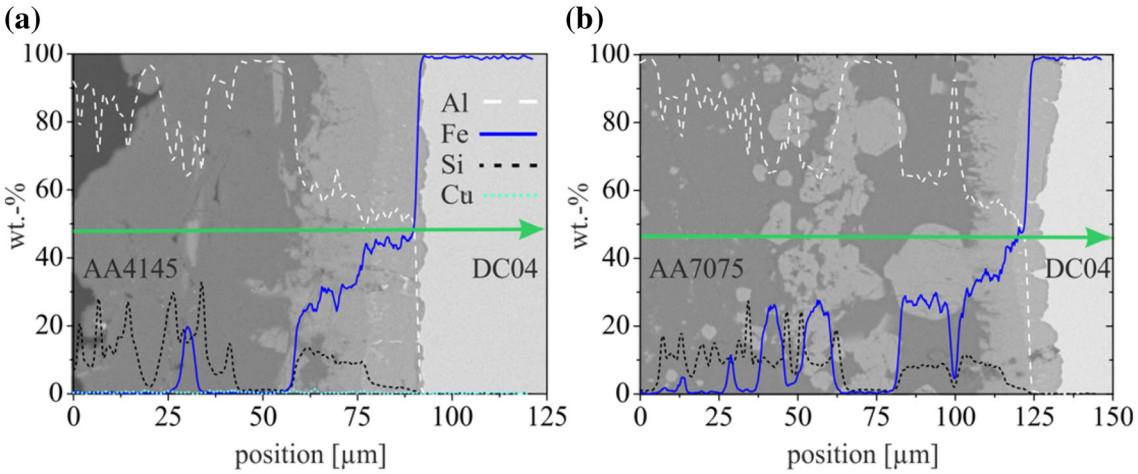

Figure 6. Line scan of the atomic fraction profile at the interface between steel DC04 and (a) AA4145 coating, (b) AA7075 coating; both after an immersion time of $t = 5$ min.

XRD Analysis

The intermetallic phases at the interface between the steel substrate and the coatings for the samples immersed in the aluminum melt at $T = 610$ °C were also analyzed by means of XRD analysis. The measurements were done on the surface of the reaction zone after it was detached from the steel substrate by pulling it off with an affixed stamp. It was proven by metallographic analysis that the coating was separated at the interface between steel and intermetallic compound for all samples. For the AA4145 coating, the Al_2Cu intermetallic phase could be detected after short immersion times of $t = 30$ s and $t = 1$ min, Figure 7. With an increasing immersion time, Al_5Fe_2, $Al_9Fe_2Si_2$ and Al_5FeSi intermetallic phases can be identified, while the intensity of the signal for copper-rich intermetallic phase gets weaker. For AA7075 alloy, the XRD results revealed the formation of Al_5Fe_2 and Al_8Fe_2Si intermetallic phases after immersion at $T = 610$ °C for $t \geq 1$ min, Figure 7. With increased immersion time, the reaction zone grows, thus leading to the reduction of the intensity of the aluminum patterns, due to the limited penetration of the XRD signal through the intermetallic phases. At the same time, the intensity of patterns of the AlFeSi and AlFe intermetallic phases increases. In comparison with the EDS analysis data, some discrepancies in the phase identification could be noticed. It can be assumed that not all intermetallic phases could be determined possibly due to the limited penetration depth of the X-ray.

Hardness Measurement

The hardness of the intermetallic phases was investigated for a better understanding of the structure and mechanical properties of the reaction zone. The hardness of the phases at the interface between coating and steel is represented in Figure 8. For the AA7075 alloy, the hardness values considerably decrease in the region between continuous and flaky layer observed at SEM micrographs.

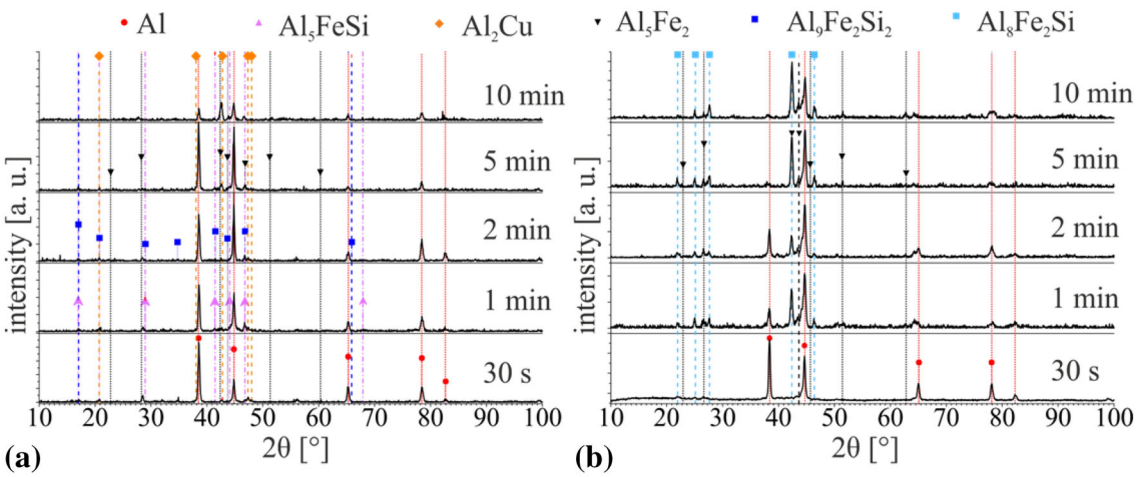

Figure 7. Diffraction patterns of the reaction zone at the interface between steel DC04 and (a) AA4145 coating, (b) AA7075 coating after different immersion times.

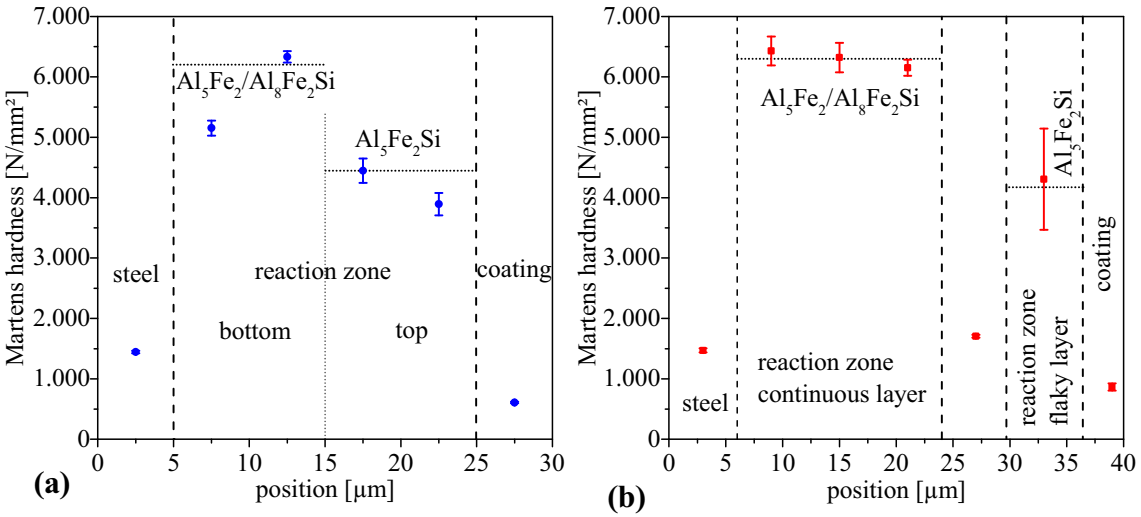

Figure 8. Martens hardness of the reaction zone after $t = 5$ min immersion at the interface between steel DC04 and (a) AA4145 coating, (b) AA7075 coating.

The maximal hardness of about HM = 6300 N/mm^2 for both coating alloys was measured in the reaction zone close to the interface between coating and steel. In accordance to the EDS analysis, XRD data and to the hardness values reported in the literature,[12] the formation of the Al_5Fe_2 phase can be assumed for this region. However, the microhardness of Al_8Fe_2Si is in a similar range,[13] so that it is difficult to separate Al_5Fe_2 and Al_8Fe_2Si phases in the continuous layer of the reaction zone for AA7075 coating by means of hardness profile. The hardness of the flaky layer of the AA7075 reaction zone as well as the hardness of the top layer of the AA4145 reaction zone corresponds to that of Al_5FeSi intermetallic phase in the literature.[13]

Formation and Growth Kinetics of the Intermetallic Phases

The growth kinetics of the intermetallic compounds was investigated by measurement of the reaction zone thickness. The average thickness of the intermetallic phase is plotted as a function of the square root of time for both, immersion in aluminum melt and for heat treatment in the fluidized sand bath. The relationship between the thickness of the whole reaction zone as well as particular layers with the square root of time can be described by means of linear regression, as all measurement points can be fitted to a strain line with the minimal coefficient of variation $R^2_{min} = 0.89$, Figure 9. Therefore, the thickness of the intermetallic compound d can be described as:[12,14]

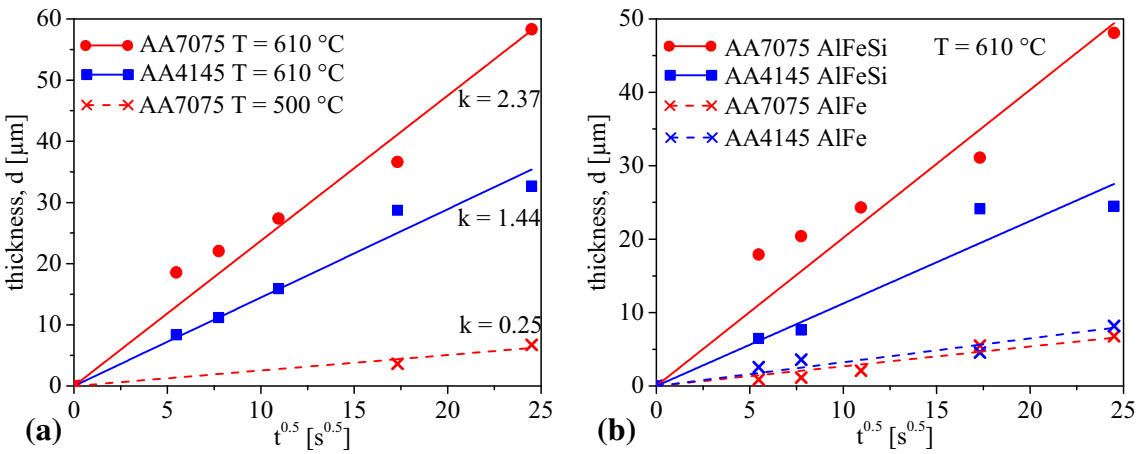

Figure 9. Mean thickness of a reaction zone after immersion at $T = 610$ °C and heat treatment at $T = 500$ °C with coefficient of growth k, µm/s$^{0.5}$, (b) Al_xFe_y layer and $Al_xFe_ySi_z$ layer after immersion at $T = 610$ °C.

$$d = k \cdot t^{0.5} \qquad \text{Eqn. 2}$$

In accordance with Eqn. 2, the slope of the lines corresponds to the parabolic coefficient k. As the growth behavior of the intermetallic phases can be described by a parabolic law, it can be assumed to be diffusion controlled. After the heat treatment at $T = 500$ °C, no intermetallic phases were detected for AA4145 coating and only a thin reaction zone with a thickness of about $d_{RZ} = 4$ µm has formed at the interface between AA7075 coating and steel substrate after heat treatment time of $t = 5$ min. For the immersion in the aluminum melt at $T = 610$ °C, the parabolic coefficient of the reaction layer growth calculated from measured at SEM micrographs was almost 5 times higher comparing to that during heat treatment, Figure 9a. The thickness measurement on SEM micrographs has shown that the area of the whole reaction zone, formed at the interface between coatings and steel during the immersion in the aluminum melt was larger in the case of AA7075 alloy, which can be seen in Figure 9a. However, the direct comparison of the growth kinetics is difficult due to the totally different morphology of the intermetallic layers for both coatings. In Figure 9b, the mean thickness of the AlFe and AlFeSi layers after immersion is shown for both coatings. A thin layer of AlFe formed at the interface between steel and coatings, growing much slower than the AlFeSi one. The growth rates of the AlFe layer are comparable for both coatings. However, the AlFeSi layer grows noticeably faster in the case of AA7075. The Al_8Fe_2Si phase is reported to be the dominant intermetallic layer forming by reaction of the silicon containing aluminum melt and steel followed by the Al_5FeSi phase,[9] which was also observed in the current study.

In Table 5, an overview of the data about the estimated values of the coefficient k reported in the literature is given. Only information on similar material couples and similar temperature ranges is considered here. The studies of Springer et al.[15,16] show that adding Si to Al melts results in a reduced growth rate of the reaction layer in a solid/liquid interdiffusion process as compared to pure Al melts, which conforms with other well-known results from the literature.[7,17,18] Deceleration of the intermetallic layer growth has been shown in the study of Takata et al.[19] by a simultaneous addition of Si and Mg in aluminum melt. However, for a heat treatment at $T = 500$ °C and $T = 600$ °C, i.e., for a solid state reaction of steel and aluminum, the opposite effect of Si was observed in Reference 15. Parabolic coefficient k measured in the current study for AA7075 coating at the temperature $T = 500$ °C ($k = 0.25$ µm/s$^{0.5}$) is similar to that calculated in Reference 15 for friction stir-welded AlSi5/DC01 compounds annealed at $T = 500$ °C ($k = 0.201$ µm/s$^{0.5}$). Furthermore, the measured coefficients k for the samples immersed in aluminum melt with a temperature $T = 610$ °C are in the same order as presented in the study of Ei-Mahallawy et al.[20] even though the temperature of the aluminum bath in the cited work was $T = 690$ °C.

Despite different morphologies of the reaction zone for both coatings, its structure is similar, containing the same AlFeSi phases, although the coatings have different chemical composition, especially regarding the silicon content. Considering this fact, diffusion of silicon from the aluminum melt toward coating can be assumed in the case of AA7075 coating. This was proven by EDS analysis, comparing the silicon content in the coating after immersing times of $t = 30$ s and $t = 10$ min, Figure 10b, d. The measurement of the chemical composition of the coating was carried out at three different positions in the coating on a surface of $S = 50 \times 30$ µm^2. At the same time, magnesium and zinc diffuse in the opposite direction toward the aluminum melt. Several authors have shown that the formation and growth kinetics of the intermetallic compounds is described by reaction diffusion laws.[12,14] Thus, the diffusion rate of the main elements involved in the formation of intermetallic compounds can also play a vital role for their morphology. For AA4145, a similar trend can be observed regarding the copper content of the coating. With increasing immersion time, the amount of copper decreased drastically indicating copper diffusion toward aluminum melt, Figure 10a, c. Interestingly, the silicon content increases only slightly with immersion time, although the coating alloy AA4145 contains slightly more silicon in its chemical composition than the cast alloy Trimal 37. It can be assumed that the formation of AlFeSi intermetallic phases is accompanied by the reduction of the silicon content in the coating, leading to a concentration gradient between aluminum melt and coating. Thus, the diffusion of silicon in the case of AA4145 coating is also

Table 5. Comparison of the parabolic coefficients k from different studies[15,16,20]

Author	Springer et al.[15]				Springer et al.[16]	Ei-Mahallawy et al.[20]	
Steel	DC01		DC01		DC04	Low carbon steel	
Aluminum	$AlSi_5$		Al		Al	$AlSi_8$	Al
Al state	Semisolid		Solid		Solid	Liquid	Liquid
Temperature (°C)	500	600	500	600	600	690	690
k (µm/s$^{0.5}$)	0.201	2.303	0.141	0.242	0.185	1.962	3.35

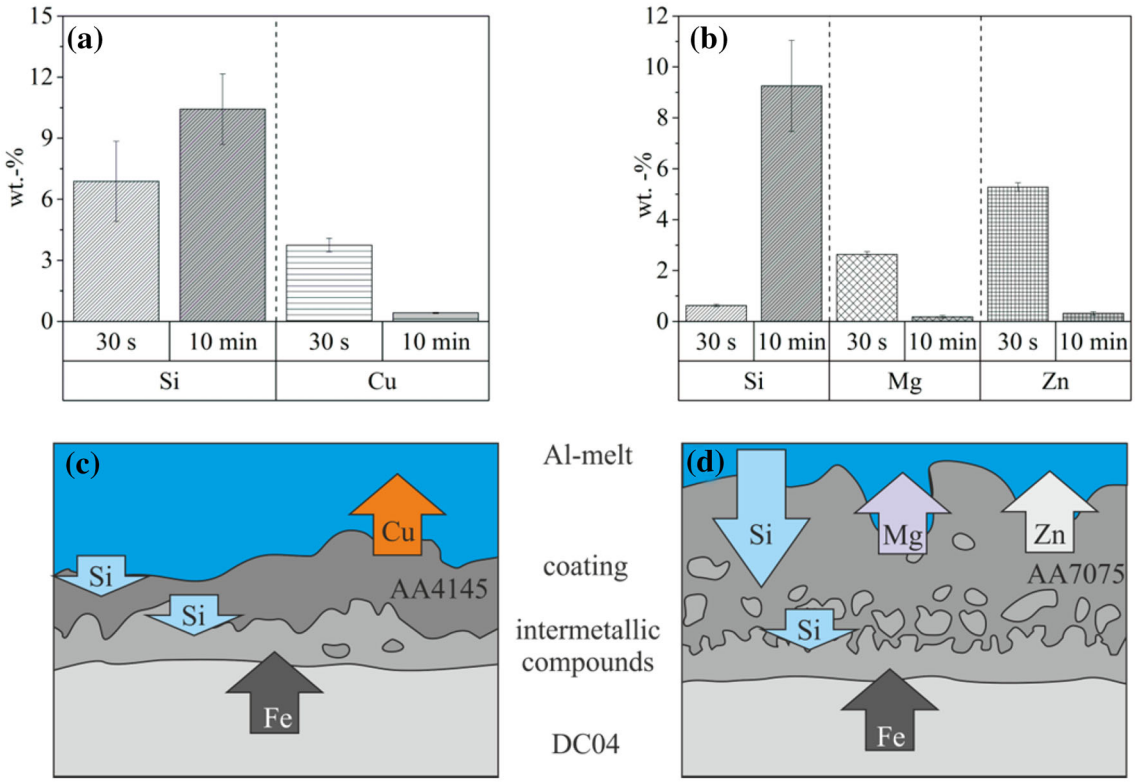

Figure 10. Silicon, copper, magnesium and zinc content of the (a) AA4145 coating, (b) AA7075 coating after immersing time of $t = 30$ s and $t = 10$ min, determined by EDS analysis and the scheme of the diffusion direction for main alloying elements of the (c) AA4145 coating, (d) AA7075 coating.

directed from cast alloy toward coating. Fragner et al.[10] have supposed that silicon diffusion is a key factor affecting the morphology and growth kinetics of AlFeSi compounds between aluminum melt and steel. The results from the current study partly corroborate this hypothesis.

Conclusion

In the current study, the kinetics of the reactive diffusion between cold gas-sprayed Al-based coatings AA4145 and AA7075 and steel DC04 was experimentally examined by means of immersion tests in aluminum melt and heat treatment in fluidized sand bath. It was shown that the reaction zone has a completely different morphology. At the same time, the composition of the reaction zones of both coatings is similar consisting of $(Al,Si)_2Fe/Al_5Fe_2$, Al_8Fe_2Si, $Al_{12}Fe_5Si$ and Al_5FeSi. Intermetallic layers were analyzed by means of EDS and XRD analysis and hardness measurement. After immersion tests, a massive diffusion of silicon from aluminum cast alloy into the coating AA7075 was detected by means of EDS analysis. Furthermore, the diffusion of Mg and Zn from AA7075 coating toward aluminum melt was observed. For AA4145 coating, the silicon content remained stable after different immersion times, while copper diffused toward aluminum melt. The different behavior of the alloying elements of the coatings can be explained by concentration gradients due to different chemical composition of the coatings and aluminum melt. For AA7075 coating, the diffusion fluxes of three main alloying elements of the coating, namely Si, Mg and Zn, are responsible for the formation and morphology of the reaction zone. For AA4145 coating, the diffusion flux between is aluminum melt and coating contains Cu and Si, however, due to the similar content for Si the diffusion of this element is not comparable to that for AA7075. Almost no reaction between coatings and steel occurred after the heat treatment in the fluidized sand bath furnace at $T = 500$ °C. In further investigations, coatings behavior during the high-pressure die casting will be investigated. The growth kinetics of AlFe and AlFeSi intermetallic layers was slower for AA4145 coating which is favorable, as the intermetallic compounds are undesirable regarding the joining of aluminum and steel. Considering the results of the heat treatment experiments at the temperature of $T = 500$ °C, it can be assumed that the reaction between steel and Al-based coatings can be avoided due to the rapid cooling after the high-pressure casting process. Furthermore, with regard to the conclusions from immersion tests, we can expect a partial melting of the AA7075 alloy which can lead to a metallurgical bonding between aluminum melt and coating.

Acknowledgements

This research is supported by the German Research Foundation (DFG) under Contract No. BO 1979/39-1. Special thanks are addressed to our project partners from the institute of metal forming (IBF) from RWTH Aachen University.

REFERENCES

1. S. Nisslé, S. Dassler, U. Noster, A. Mundl, Verbundguss, Neue Auslegungsmöglichkeiten für Gussteile durch Funktionsintegration oder lokale Verstärkung. Tagungsband der 5. Ranshofener Leichtmetalltage (LKR-Verlag, Ranshofen, 2008), pp. 35–44
2. A. Fent, Magnesium-Aluminium-Verbundkurbelgehäuse-Einsatz von Neutronen in der Bauteilentwicklung. Garching (2006)
3. C. Oberschelp, Hybride Leichtbaustrukturen für den Karosseriebau - gusswerkstofforientierte Anwendungsuntersuchungen für das Druckgießen. Diss., Gießerei-Inst. der RWTH, Aachen (2012)
4. Variostruct: multi-material-components. http://www.variostruct.de/?L=1
5. K. Bouché, F. Barbier, A. Coulet, Intermetallic compound layer growth between solid iron and molten aluminium. Mater. Sci. Eng. A **249**(1-2), 167–175 (1998)
6. W.-J. Cheng, C.-J. Wang, EBSD study of crystallographic identification of Fe–Al–Si intermetallic phases in Al–Si coating on Cr–Mo steel. Appl. Surf. Sci. **257**(10), 4637–4642 (2011)
7. W. Fragner, B. Zberg, R. Sonnleitner, P.J. Uggowitzer, J.F. Löffler, Interface reactions of Al and binary Al-alloys on mild steel substrates in controlled atmosphere. MSF **519–521**, 1157–1162 (2006)
8. Y. Tanaka, M. Kajihara, Morphology of compounds formed by isothermal reactive diffusion between solid Fe and liquid Al. Mater. Trans. **50**(9), 2212–2220 (2009)
9. K.A. Nazari, S.G. Shabestari, Effect of micro alloying elements on the interfacial reactions between molten aluminum alloy and tool steel. J. Alloy. Compd. **478**(1-2), 523–530 (2009)
10. W. Fragner, K. Papis, J. Wosik, P.J. Uggowitzer, Herausforderungen und Lösungsmöglichkeiten bei der Herstellung von Verbundgussteilen. Vortragstext, 5. Ranshofener Leichtmetalltage 2008, LKR-Verlag, herausgegeben von U. Noster, F. Riemelmoser u. P. J. Uggowitzer, Ranshofen (2008), pp. 75–85
11. B. Lao, Druckgegossene Metallhybridstrukturen für den Leichtbau-Prozess, Werkstoffe und Gefüge der Metallhybriden. Diss., Gießerei-Inst. der RWTH, Aachen (2013)
12. S. Kobayashi, T. Yakou, Control of intermetallic compound layers at interface between steel and aluminum by diffusion-treatment. Mater. Sci. Eng. A **338**(1-2), 44–53 (2002)
13. V. Zolotorevski, N.A. Belov, M.V. Glazoff, *Casting aluminum alloys* (Elsevier, Oxford, 2007)
14. V.I. Dybkov, Interaction of 18Cr-10Ni stainless steel with liquid aluminium. J. Mater. Sci. **25**(8), 3615–3633 (1990)
15. H. Springer, A. Kostka, J.F. dos Santos, D. Raabe, Influence of intermetallic phases and Kirkendall-porosity on the mechanical properties of joints between steel and aluminium alloys. Mater. Sci. Eng. A **528**(13-14), 4630–4642 (2011)
16. H. Springer, A. Kostka, E.J. Payton, D. Raabe, A. Kaysser-Pyzalla, G. Eggeler, On the formation and growth of intermetallic phases during interdiffusion between low-carbon steel and aluminum alloys. Acta Mater. **59**(4), 1586–1600 (2011)
17. B. Lemmens, H. Springer, I. de Graeve, J. de Strycker, D. Raabe, K. Verbeken, Effect of silicon on the microstructure and growth kinetics of intermetallic phases formed during hot-dip aluminizing of ferritic steel. Surf. Coat. Technol. **319**, 104–109 (2017)
18. W.-J. Cheng, C.-J. Wang, Effect of silicon on the formation of intermetallic phases in aluminide coating on mild steel. Intermetallics **19**(10), 1455–1460 (2011)
19. N. Takata, M. Nishimoto, S. Kobayashi, M. Takeyama, Morphology and formation of Fe–Al intermetallic layers on iron hot-dipped in Al–Mg–Si alloy melt. Intermetallics **54**, 136–142 (2014)
20. N.A. Ei-Mahallawy, M.A. Taha, M.A. Shady, A.R. Ei-Sissi, A.N. Attia, W. Reif, Analysis of coating layer formed on steel strips during aluminising by hot dipping in Al-Si baths. Mater. Sci. Technol. **13**(10), 832–840 (2013)